Fusion Engineering and Design, Volume 149, December 2019, 111329, ISSN 0920-3796,

https://doi.org/10.1016/j.fusengdes.2019.111329

Design, mechanical analysis and manufacturing of the IFMIF LIPAc beam dump shielding

Oriol Nomen [a], Beatriz Brañas [b], Fernando Arranz [b], Francisco Ogando [c], Jesús Castellanos [b], Joseba Balerdi [d]

[a] *IREC, Catalonia Institute for Energy Research, Jardins de les Dones de Negre 1, 08930 Sant Adrià de Besòs, Catalonia, Spain*

[b] *CIEMAT, Avenida Complutense, 40, 28040 Madrid, Spain*

[c] *UNED, C/ Juan del Rosal 12, 28040 Madrid, Spain*

[d] *CADINOX, Okobio, 32, 20491 Belauntza, Basque Country, Spain*

Abstract

The International Fusion Materials Irradiation Facility (IFMIF) aims to provide an accelerator-based, D-Li neutron source to produce high energy neutrons at enough intensity and irradiation volume for DEMO materials qualification. As part of the Broader Approach (BA) agreement between Japan and EURATOM, the goal of the IFMIF/EVEDA project is to work on the engineering design of IFMIF and to validate the main technological challenges which, among a wide diversity of hardware includes the LIPAc (Linear IFMIF Prototype Accelerator), a 125 mA continuous wave deuteron accelerator up to 9 MeV mainly designed and manufactured in Europe.

The beam is stopped in a copper cone involving a high production of neutron and gamma radiation and activation of its surface. A shield has been designed to attenuate both the radiation produced during accelerator operation and the residual radiation. This shield is made of an inner layer of polyethylene to moderate neutrons and an outer layer of iron to attenuate gammas produced by deuteron interactions with Cu but also those generated by neutrons in the polyethylene.

The present work summarizes the upgraded design of the shielding, as well as its upgraded mechanical analysis following the ASME Boiler and Pressure Vessel Code Division VIII Section 2. It also shows the manufacturing processes and requirements imposed on the shielding along with the acceptance tests performed and the lessons learned.

Keywords:

IFMIF, LIPAc, Beam dump shielding, Mechanical design, Mechanical analysis, Manufacturing

1. Introduction

The International Fusion Materials Irradiation Facility, also known as IFMIF, will be a test facility for the qualification of fusion reactors candidate materials [1]. The LIPAc (Linear IFMIF Prototype Accelerator) [2,3] is a prototype accelerator (9 MeV, 125 mA of D + beam in continuous wave), identical to the low energy part of one of the two IFMIF accelerators.

The LIPAc will not have a target and hence a dump is needed to stop the deuteron beam [4,5]. The beam will be stopped by a copper cone (2.5 m long, 6.8° angle), cooled by water flowing at high velocity along its outer surface. The system containing the copper cone and its cooling is called beam dump cartridge.

Due to the interaction of the 9 MeV deuterons with the copper, both neutrons and gammas are generated. The copper cone is surrounded by a shield which has been designed to attenuate both the radiation produced during accelerator operation and the residual radiation [[6], [7], [8]]. This shield (see Fig. 1) is made of an inner layer of polyethylene to moderate neutrons and an outer layer of iron to attenuate gammas produced by deuteron interactions with Cu but also those generated by neutrons in the polyethylene. In the central part surrounding the cartridge the thicknesses of the polyethylene and iron layers are 45 cm and 25 cm respectively.

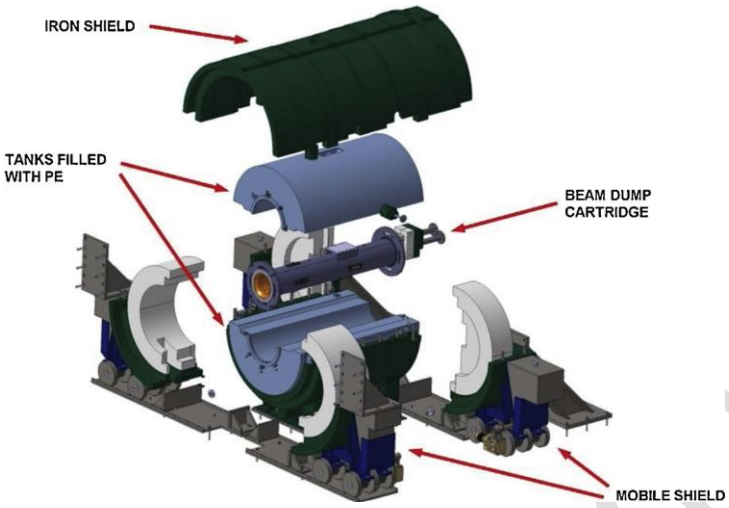

Figure 1 Components of the beam dump shielding.

At the front side (towards the accelerator), the shielding is closed with a 700 mm thick, 3 m high concrete wall which separates the space where the beam dump is located (called beam dump cell) from the rest of the accelerator vault. This wall has a cylindrical hole for the passage of the beam tube.

The shield and the concrete wall surround the beam dump completely except at the entrance of the beam line. During maintenance this entrance will be covered by a lead shutter [7,9] to prevent the beam dump residual radiation from reaching the vault (see Fig. 2).

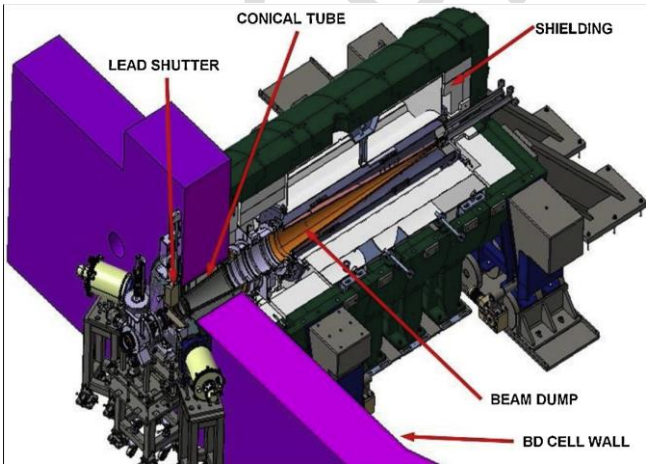

Figure 2 Quarter section of the beam dump showing all shielding elements.

Fig. 1 shows an exploded view of the beam dump shield, containing the outer iron shield and the inner polyethylene shield, surrounding the beam dump cartridge.

The central part of the polyethylene shield has been encapsulated in aluminum tanks. The frontal and rear parts of the shield are mounted in movable trolleys to allow access to the cartridge flanges and to the connection with the accelerator line.

2. Requirements

The main requirement of the shield is to attenuate both the radiation produced during accelerator operation and the residual radiation. Other requirements including reduced own contribution to radiation, structural integrity, dimensional tolerances, alignment capability, commissioning, decommissioning and regulation have been considered.

The components of the shield must be recyclable at the end of the life of the beam dump, avoiding their processing in a warehouse of radioactive waste. This is the reason why aluminum has been chosen for the tanks. Limits in impurity concentrations must be fulfilled in the aluminum, and so, the content in parts per million (ppm) in weight of Zn, Co and Cs must be lower than 90–550 (depending on the region of the tank), 5 and 3.8, respectively. After a search and procurement of the raw material was done, it became apparent that the impurity which contributed most to activation was the Zn from which Zn65 is produced. The Zn content in the inner region of the tanks is 90 ppm. Assuming a lifetime of the facility of 0.5 fpy, where fpy means full-power year, the aluminum tank will be recyclable after 6 months of cooling. The content of Co in the iron shield must be lower than 1000 ppm, ensuring a minimum impact of the contribution of the shielding activation to the total dose rate when the beam is off.

Taking into account that, due to the residual doses from the cartridge, maintenance is not possible in the components inside the shielding and that the initial design of the tanks had a strict requirement for water leak tightness since the tanks were proposed to be filled with water [7], the structural assessment of the components of the shielding was implemented following the ASME Boiler and Pressure Vessel Code Division VIII Section 2 [10] and applying the following loads:

- Own weight of the part to be analyzed.
- For seismic validation, according to [11], accelerations of 0.4 g in horizontal direction and 0.2 g in vertical direction (where g is the acceleration of gravity), as equivalent solicitations for a quasi-static analysis.
- Reactions in the upper parts, if applicable (as explained in paragraph 3.2 of [7]).

The beam dump cartridge must be aligned with an accuracy better than ±0.1 mm while supported in the beam dump shielding. So, the dimensional tolerances of the components of the shielding and the regulation capability for positioning the different components must ensure the achievement of the required alignment accuracy.

Concerning commissioning and decommissioning requirements, the bridge crane of the accelerator building can lift a limited weight of 48 kN (Fig. 3). Its axis of displacement, parallel to the building walls is 20° apart from the beam dump shield axis. During installation and commissioning operations, hands-on maintenance is possible in the components, but after 13 days of operation at 1% duty cycle the residual doses from the cartridge prevent hands-on maintenance operations inside the shield. Removal of the upper shield must be done remotely while, after the disposal of the beam dump cartridge into a lead container, the rest of components can be managed with hands-on operations. For the aluminum tanks, the impurity limits described at the beginning of this section were defined to allow the recycling of the material even in its most irradiated regions resulting also in a limitation of the residual doses around the component during dismantling. With regard to the low alloy steel and after 6 months of cooling, the most relevant isotopes contributing to the doses are Fe59, Mn54 and Co60. The contact dose calculated in the worst point is 24 μSv/h, demonstrating that hands-on maintenance is possible.

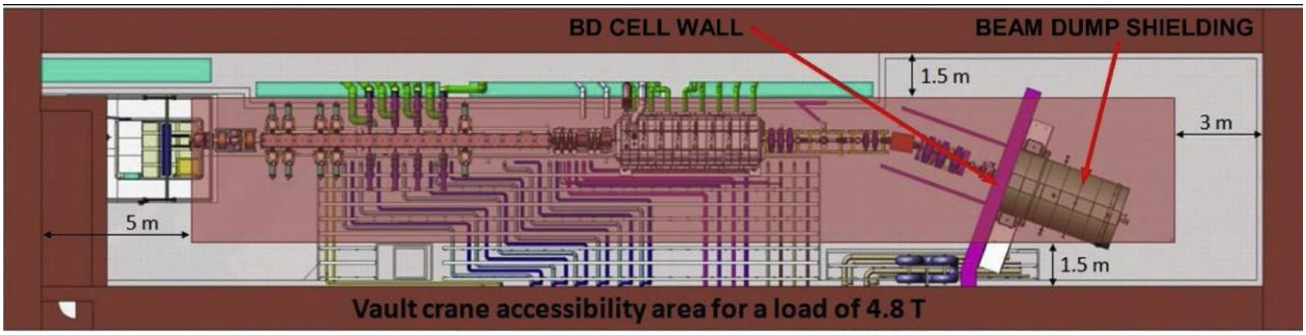

Figure 3 Top view of the vault crane accessibility.

Regarding the standards for design, manufacturing and testing, the whole process of manufacturing of the components of the shielding must follow the specifications of the ASME Boiler and Pressure Vessel Code.

3. Detailed mechanical design

The current design of the beam dump shielding has been upgraded from the former design [7]. The different components of the shielding are described in the next sections.

3.1. Aluminum tanks filled with polyethylene

The former design [5,7] with two tanks enclosing the Beam Dump cartridge in the central part and a tank in the rear part has been changed substituting the rear tank by polyethylene pieces fixed to the iron shielding and mounted on a mobile trolley. These mobile trolley allows the access to the rear flange of the beam dump cartridge (Section 3.3).

The previous design was conceived with water inside the aluminum tanks as neutron shielding. To avoid any risk of leak, given that maintenance is not possible, it has been decided to use solid polyethylene, which has a shield efficiency similar to that of water, instead. Therefore, the aluminum tanks have been filled with polyethylene half ring pieces of different dimensions, ensuring no direct streaming of radiation in radial direction (Fig. 4). The aluminum chosen for the tanks is the Al 5083 alloy while the pieces filling the tanks are made of a high density polyethylene, named PE-HMW 500.

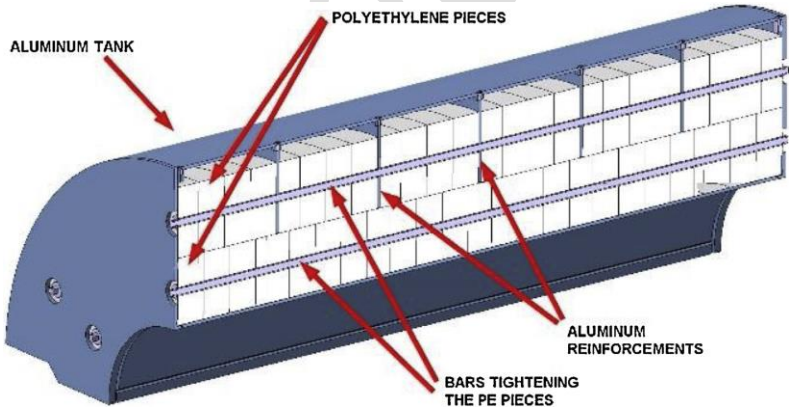

Figure 4 Polyethylene tanks.

The lower tank is fixed to the lower iron shielding with 4 supports and it sits on a lower iron beam whose vertical position can be adjusted to allow the regulation of the tank position in vertical direction (Fig. 5). The upper tank is positioned with respect of the lower tank with the aid of two holes in the lower tank and two pins in the upper tank (Fig. 6).

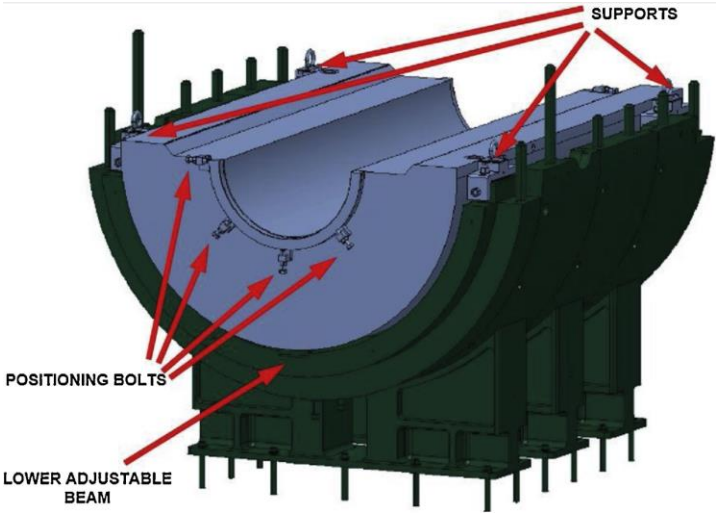

Figure 5 Supports, lower adjustable beam for the lower tank and positioning bolts for the beam dump cartridge.

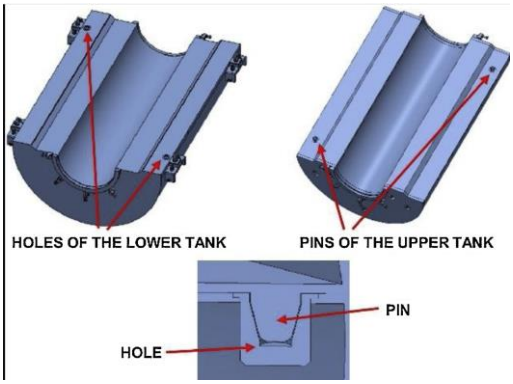

Figure 6 Holes and pins for defining the relative position of the tanks.

The upper tank contains a hook on its upper position in order to be remote handled during decommissioning (Fig. 7)

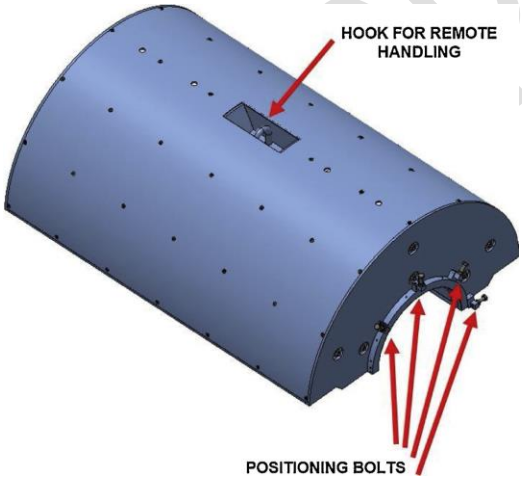

Figure 7 Hook in the upper tank for remote handling.

Both lower and upper tank contain positioning bolts in the front and rear part (Fig. 5, Fig. 7) where the beam dump cartridge is supported and can be aligned.

3.2. Fixed iron shielding

The material of the iron shielding is the low alloy steel S235. This material has been chosen instead of the originally planned gray cast iron EN-GJL-200 because of its ductile behavior, availability of raw materials in thick plate formats and absence of porosity inside the material.

The fixed shielding has been divided in half rings (4 in the upper part and 4 in the lower part) each with a mass lower than 4800 kg to allow their handling with the bridge crane of the accelerator building. The interface between neighboring half rings has been designed with a dogleg shape, to prevent radiation streaming in radial direction (Fig. 8). Each half ring contains a flat surface at the top to be transported remotely with an electromagnet.

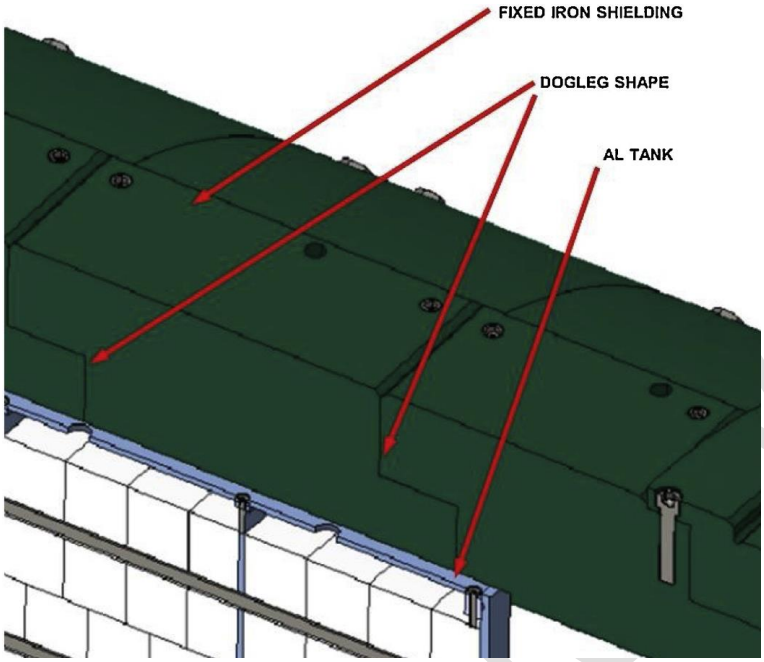

Figure 8 Dogleg shape in the half rings of the iron shielding.

3.3. Mobile shielding

In the front and rear part of the shielding, the polyethylene and iron pieces of the shielding are fixed to mobile trolleys. These trolleys can be displaced perpendicularly to the beam dump axis, opening the shield and allowing the access to the beam dump cartridge flanges (Fig. 9).

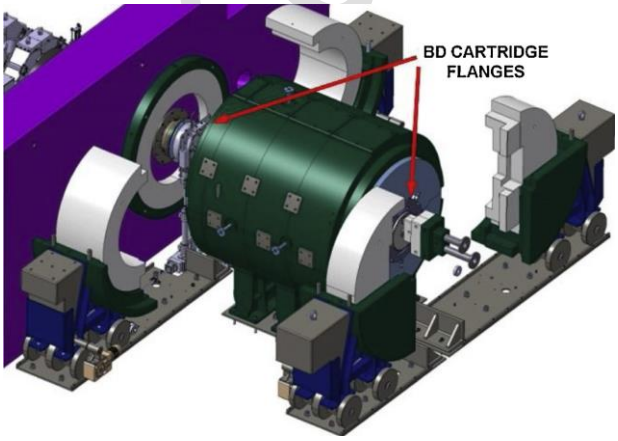

Figure 9 Access to the beam dump cartridge flanges.

Each of the trolleys is moved with a gear motor. These gear motors are dismountable, so they can be removed during the operation of the accelerator, to avoid their irradiation. The gear motors are controlled by an external console, which allows to operate the movement of the mobile trolleys from outside the beam dump cell wall. Limit switches are installed in the base plates on top of which the trolleys move, to ensure that they stop at their limit positions.

The design of the shielding in its contact with the beam dump cell wall and in the passage of the water pipes of the beam dump cartridge has been made with dogleg shapes in order to prevent or reduce radiation streaming through the interface (Fig. 10). The dogleg shape design implies that a ring containing polyethylene and iron is attached to the beam dump cell wall and another piece of polyethylene and iron is attached to the beam dump water pipes.

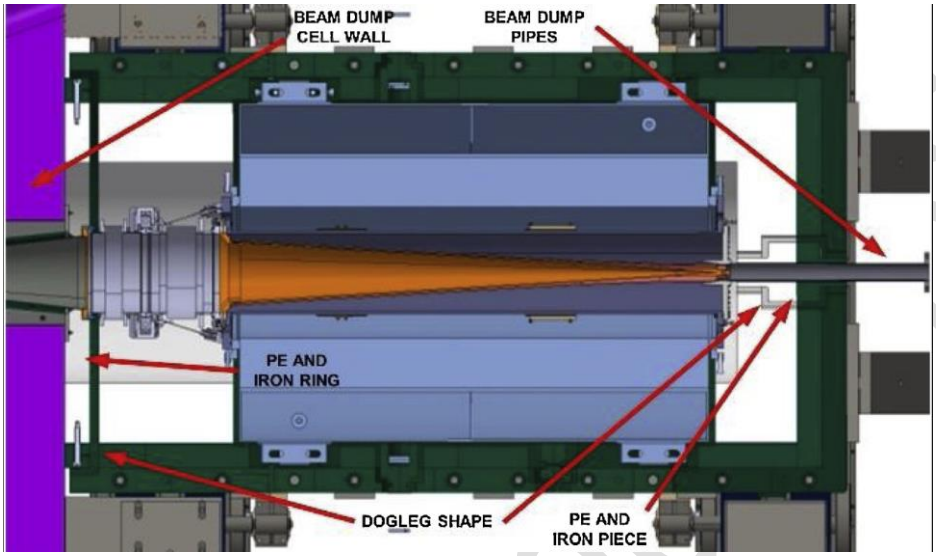

Figure 10 Dogleg shapes in the beam dump cell wall and in the passage of beam dump cartridge pipes.

During operation the trolleys are fixed to the beam dump cell wall and to the floor with structural supports. At the level of the base plates, the trolleys are also fixed with stoppers. These supports and stoppers guarantee the mobile trolleys stability in case of a seismic event (Fig. 11)

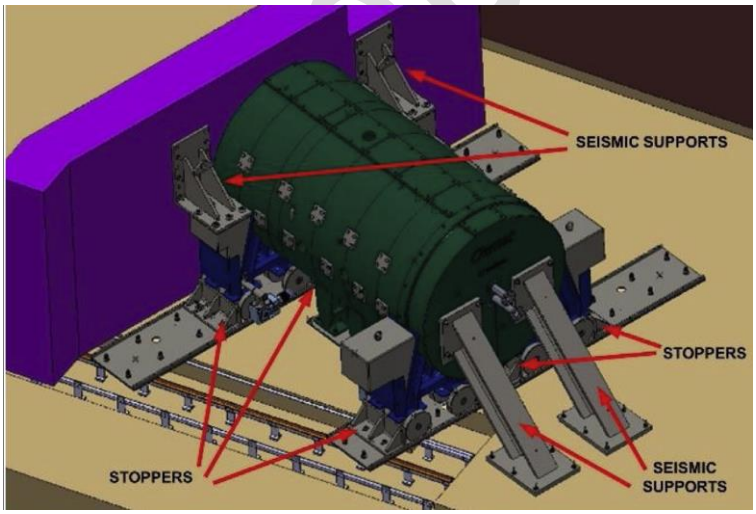

Figure 11 Seismic supports and stoppers of the mobile trolleys.

3.4. Base plates

The shield is laid on top of three base plates that ensure a good leveling independently of the flatness of the concrete floor. Each of the plates contains several leveling bolts in order to level the plate in the horizontal plane and to level all the plates among them (Fig. 12).

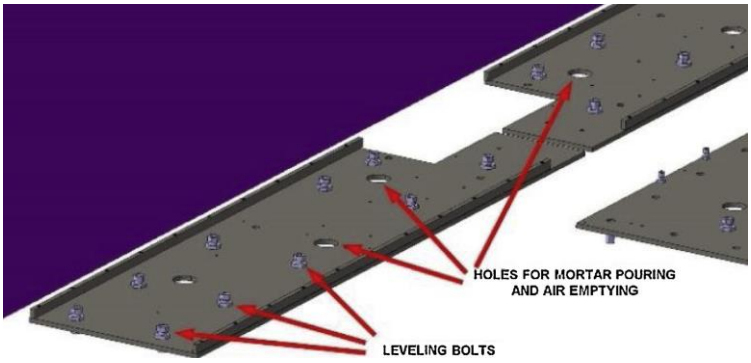

Figure 12 Levelling of the base plates and holes for mortar pouring and air emptying.

Once the levelling is done, the space between the plate and the floor is filled with a mortar in order to fix the position and to distribute the weight of the shielding in a uniform way through the plates and the floor. Holes for mortar pouring and emptying air during the operation have been machined in the plates (Fig. 12).

4. Mechanical analyses

The mechanical analyses of the former design [7] have been updated for the final design following the ASME Boiler and Pressure Vessel Code Division VIII Section 2 [10] and applying the requirements explained in Section 2.

Components have been assumed to be at room temperature (20 °C) since the beam power is evacuated by a 108 m^3/h water flow and thus the cartridge temperature at its interface with the shield is always lower than 40 °C. On the other hand, the nuclear heating in the shield materials is low. Total heat due to neutron and gamma radiation in the tanks is 170 W. The maximum nuclear heating occurs at the inner shield layers of polyethylene and it is always less than 0.3 W/kg and the shield has a large surface to evacuate this heat. A thermal analysis performed using conservative hypotheses shows that the maximum temperature increase will be less than 10 °C. Therefore, this nuclear heating has been considered negligible and has not been taken into account in the analysis.

The neutron flux expected outside the cartridge is of the order of 1010 $n \cdot cm^{-2} \cdot s^{-1}$ with an average energy of 3 MeV. This flux will result in a damage to the materials of less than 10^{-2} dpa/fpy. Given that the assumed lifetime of the machine is 0.5 fpy, the damage will be less than of 5×10^{-3} dpa. Therefore, the irradiation effects on the metallic materials of the shielding have been assumed to be negligible.

Regarding plastic materials, the maximum absorbed dose rates are of the order of 350 Gy/h (neutrons) and 800 Gy/h (gammas), giving a total absorbed dose after 6 months at full power of 5 × 106 Gy.

A limit of 10^6 Gy is established for the use of PE Cestilene HD 500 [12] which is equivalent to the PE used in this application. Going into the details, the authors have irradiated the material up to 3.4×10^6 Gy and, at that dose, the deformation of the material was reduced. In this case, as the PE does not have a structural function, apart from supporting its own weight, there is no concern about irradiation induced mechanical damage.

According to [10] and using the elastic stress analysis method, the protection against plastic collapse must fulfil the following equations:

$P_m \leq S$ (1)

$P_{\_L} \leq 1.5 \cdot S$ (2)

$(P_{\_L} + P_{\_b}) \leq 1.5 \cdot S$ (3)

P_m represents the general primary membrane equivalent stress, P_b the primary bending equivalent stress and P_L the local primary membrane equivalent stress, while S is the allowable stress of the material.

Linearization of stresses has been applied in several lines of the components where the equivalent stresses reach their maximum values. To evaluate protection against plastic collapse, the computed equivalent stresses have been compared to their corresponding maximum allowable values, according to Eqs (1), (2) and (3).

The worst case loads for each part of the shielding are being explained and shown in the next sections. Values appearing in the next sections for the allowable stress S are referred to the low alloy structural steel S235 for S = 118 MPa, to the aluminum alloy Al 5083 H112 for S = 78.6 MPa and to the austenitic stainless steel 316 L for S = 115 MPa.

4.1. Upper iron shielding

The mesh has been carried out with second order hexahedral elements and element size 15 mm, resulting in 1094136 nodes and 279872 elements.

Apart from the loads already explained in Section 2, the boundary conditions for this analysis comprise compression only supports in the base of the upper iron shielding, in order to simulate the contact with the lower shielding, and fixed supports in the holes where the bolts of the connecting plates are placed, in order to simulate that these connecting plates fix together the upper and lower shielding. The two upper half rings of the analysis have been coupled by a perfect contact model.

The maximum equivalent Von Misses stress experienced by the half rings is 11.2 MPa and the maximum deformation experienced is 0.01 mm (Fig. 13).

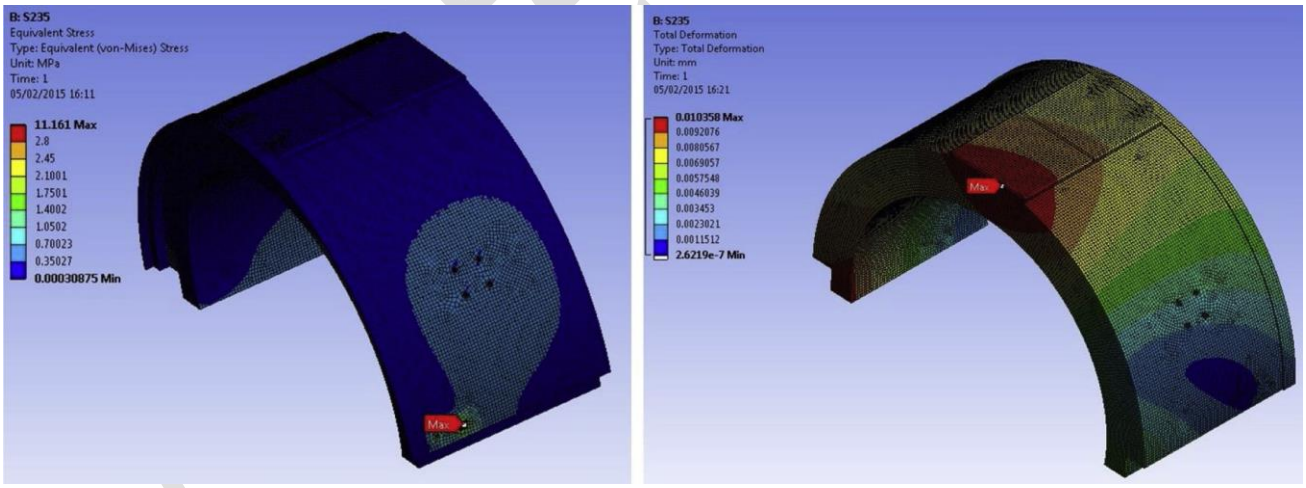

Figure 13 Von Misses stress and total deformation at the upper iron shielding.

Linearization of stresses has been applied in 5 lines of the upper iron shielding as shown in Fig. 14. The results are shown in Table 1, where the Safety Factor is the ratio between the Allowable Stress and the Stress Load. All the lines fulfil the requirements of the ASME code.

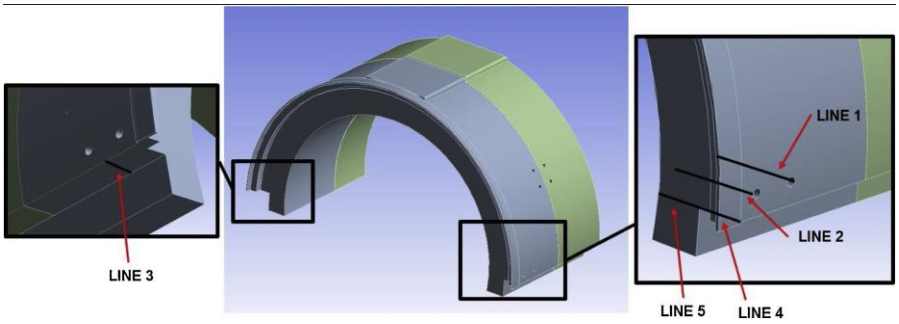

Figure 14 Lines where linearization of stresses has been applied in the upper shielding.

Table 1 Evaluation of protection against plastic collapse for the upper shielding.

Line	Stress Load	Allowable Stress	Safety factor
1	P_m=2.2 MPa	S=118 MPa	56.6
	P_L+P_b=6 MPa	1.5S=177 MPa	29.5
2	P_m=0.6 MPa	S=118 MPa	196.7
	P_L+P_b=1.6 MPa	1.5S=177 MPa	110.6
3	P_m=0.3 MPa	S=118 MPa	393.3
	P_L+P_b=0.8 MPa	1.5S=177 MPa	147.5
4	P_m=0.7 MPa	S=118 MPa	168.5
	P_L+P_b=1.2 MPa	1.5S=177 MPa	147.5
5	P_m=0.4 MPa	S=118 MPa	295
	P_L+P_b=0.8 MPa	1.5S=177 MPa	221.3

4.2. Aluminum tanks

The mesh has been carried out with second order hexahedral elements and element size 10 mm, resulting in 2096392 nodes and 484413 elements.

The boundary conditions for this analysis comprise a fixed support in the footprint of the beam that positions the lower tank in the shielding and fixed supports in the bolts and the base of the 4 supports that fix the lower tank to the shielding. The different components of the lower tank have been coupled by a perfect contact model.

The maximum load for the tanks appears in the lower tank in the case that a transversal seismic acceleration of 0.4 g and a vertical seismic acceleration of 0.2 g are applied, together with the gravity force and the loads transferred by the upper tank and the beam dump cartridge.

The maximum equivalent Von Misses stress experienced by the tanks is 100.9 MPa and the maximum deformation is 0.77 mm (Fig. 15).

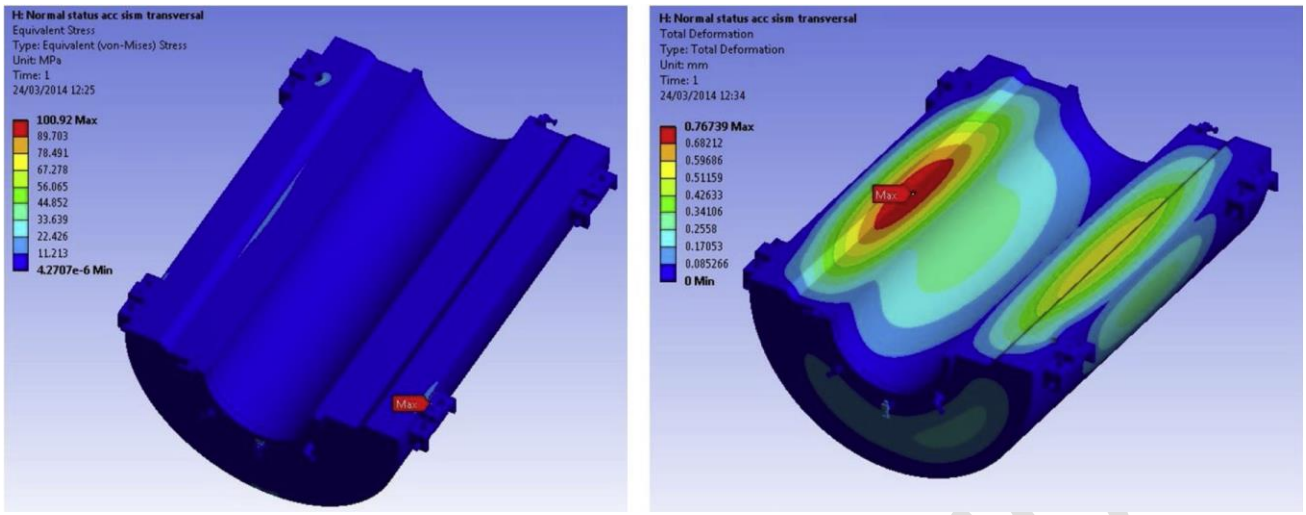

Figure 15 Von Misses stress and total deformation at the lower tank.

Linearization of stresses has been applied in 5 lines of the lower aluminum tank as shown in Fig. 16. The results are shown in Table 2, where the Safety Factor is the ratio between the Allowable Stress and the Stress Load. All the lines fulfil the requirements of the ASME code.

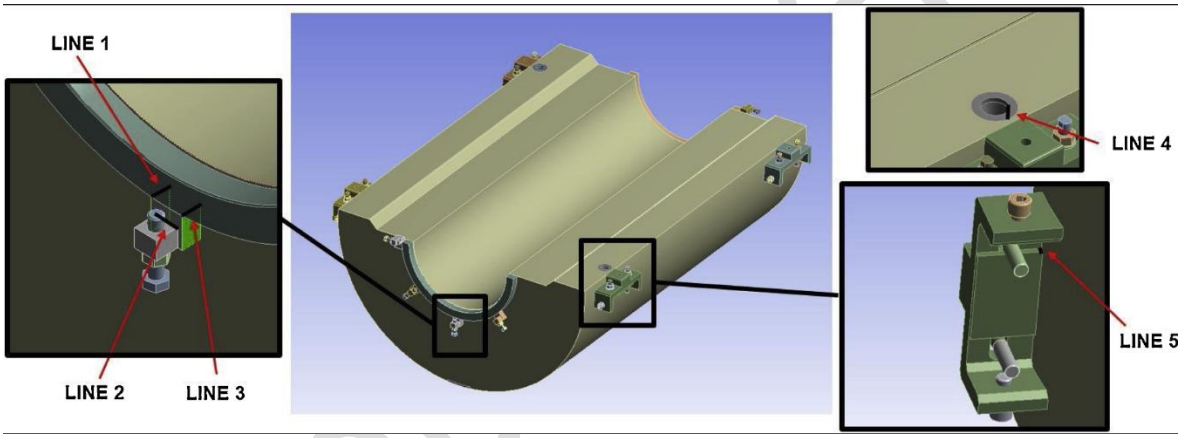

Figure 16 Lines where linearization of stresses has been applied in the lower tank.

Table 2 Evaluation of the protection against plastic collapse for the aluminum tanks.

Line	Stress Load	Allowable Stress	Safety Factor
1	P_m=13.3 MPa	S=78.6 MPa	5.9
	P_L+P_b=44.4 MPa	1.5S=118 MPa	2.7
2	P_m=29.3 MPa	S=78.6 MPa	2.7
	P_L+P_b=30.2 MPa	1.5S=118 MPa	3.9
3	P_m=13.1 MPa	S=78.6 MPa	6
	P_L+P_b=43.8 MPa	1.5S=118 MPa	2.7
4	P_m=17.1 MPa	S=78.6 MPa	4.6
	P_L+P_b=51.8 MPa	1.5S=118 MPa	2.3
5	P_m=42.2 MPa	S=115 MPa	2.7
	P_L+P_b=86.3 MPa	1.5S=172.5 MPa	2

4.3. Lower iron shielding

The mesh has been carried out with second order hexahedral elements and element size 20 mm, resulting in 1536199 nodes and 422831 elements.

The boundary conditions for this analysis comprise fixed supports in the 3 bases of the lower iron shielding feet. The different components of the lower iron shielding have been coupled by a perfect contact model.

The worst case corresponds to a transversal seismic acceleration of 0.4 g jointly applied with a vertical seismic acceleration of 0.2 g, together with the gravity force and the loads transferred by the tanks, the beam dump cartridge and the upper iron shielding.

The maximum equivalent Von Misses stress experienced by the lower shielding is 14.7 MPa and the maximum deformation experienced is 0.08 mm (Fig. 17).

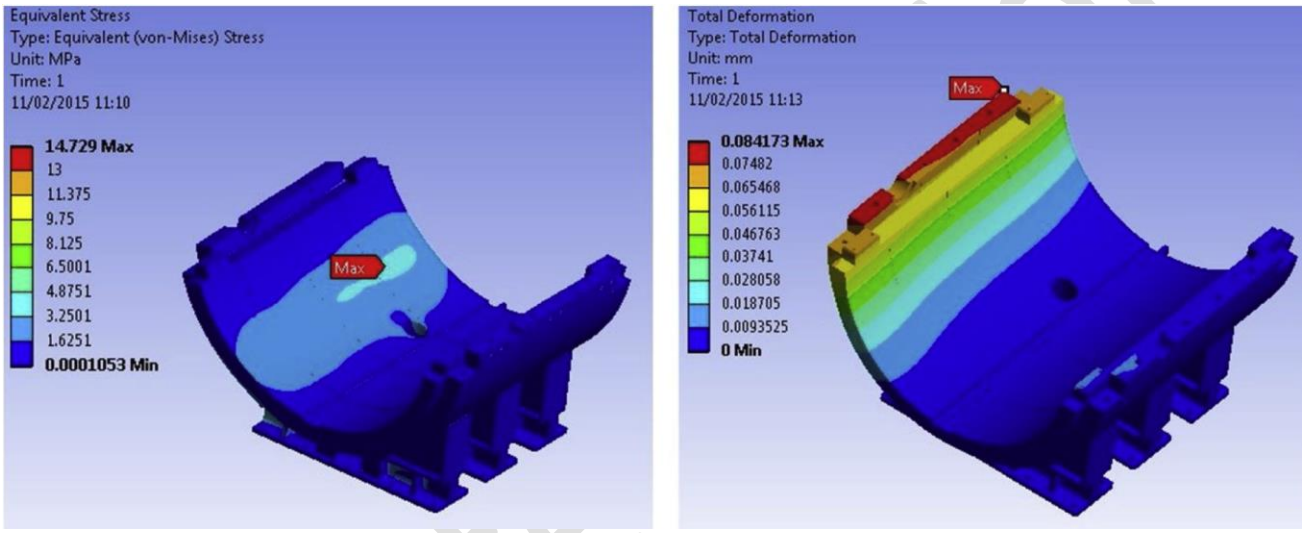

Figure 17 Von Misses stress and total deformation at the lower iron shielding.

Linearization of stresses has been done in 7 lines of the lower iron shielding as shown in Fig. 18. The results are shown in Table 3, where the Safety Factor is the ratio between the Allowable Stress and the Stress Load. All the lines fulfil the requirements of the ASME code.

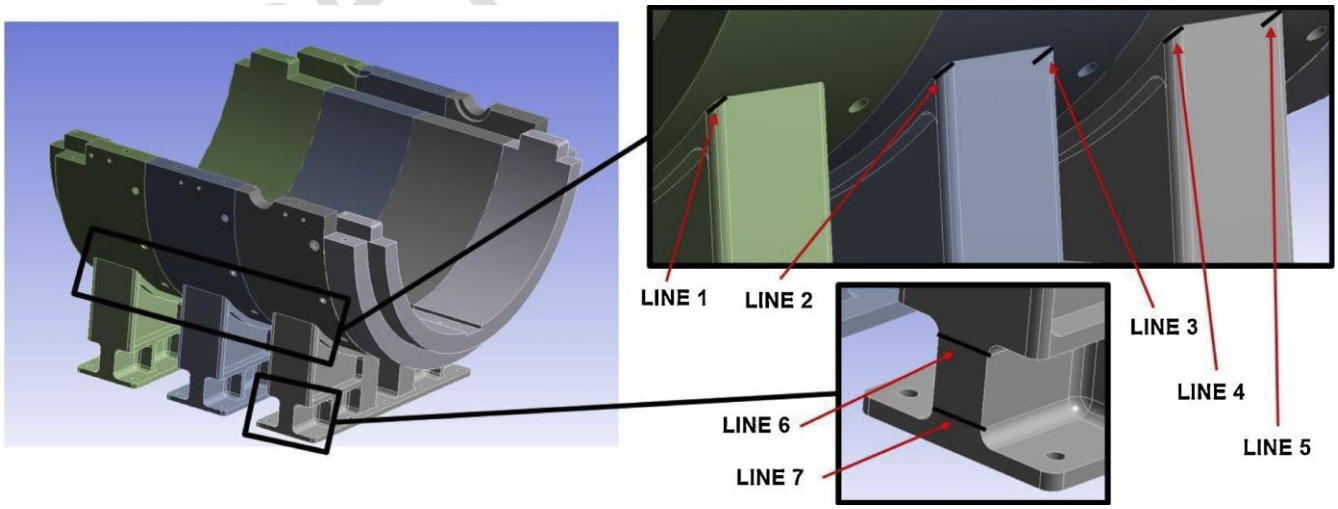

Figure 18 Lines where linearization of stresses has been applied in the lower iron shielding.

Table 3 Evaluation of protection against plastic collapse for the lower iron shielding.

Line	Stress Load	Allowable Stress	Safety factor
1	P_m=5.3 MPa	S=118 MPa	22.3
	P_L+P_b=7.6 MPa	1.5S=177 MPa	23.3
2	P_m=6.6 MPa	S=118 MPa	17.9
	P_L+P_b=8.7 MPa	1.5S=177 MPa	20.3
3	P_m=6.1 MPa	S=118 MPa	19.3
	P_L+P_b=8.2 MPa	1.5S=177 MPa	21.6
4	P_m=6.3 MPa	S=118 MPa	18.7
	P_L+P_b=8.3 MPa	1.5S=177 MPa	21.3
5	P_m=5.9 MPa	S=118 MPa	20
	P_L+P_b=8.8 MPa	1.5S=177 MPa	20.1
6	P_m=4 MPa	S=118 MPa	29.5
	P_L+P_b=4.6 MPa	1.5S=177 MPa	38.5
7	P_m=4.2 MPa	S=118 MPa	28.1
	P_L+P_b=4.7 MPa	1.5S=177 MPa	37.7

4.4. Mobile shielding

The mesh has been carried out with second order hexahedral elements and element size 25 mm, resulting in 1660913 nodes and 466214 elements.

The boundary conditions for this analysis comprise all displacements neglected except vertical displacement for the 12 wheels of the mobile trolleys and fixed supports in the holes where bolts fix together the mobile shielding with its supports to the beam dump cell wall. The different components of the mobile shielding have been coupled by a perfect contact model.

The worst load appears in the mobile front shielding in the case that a transversal seismic acceleration of 0.4 g and vertical seismic acceleration of 0.2 g are applied, together with the gravity force.

The maximum equivalent Von Misses stress experienced by the mobile front shielding is 75.2 MPa and the maximum deformation experienced is 0.16 mm (Fig. 19).

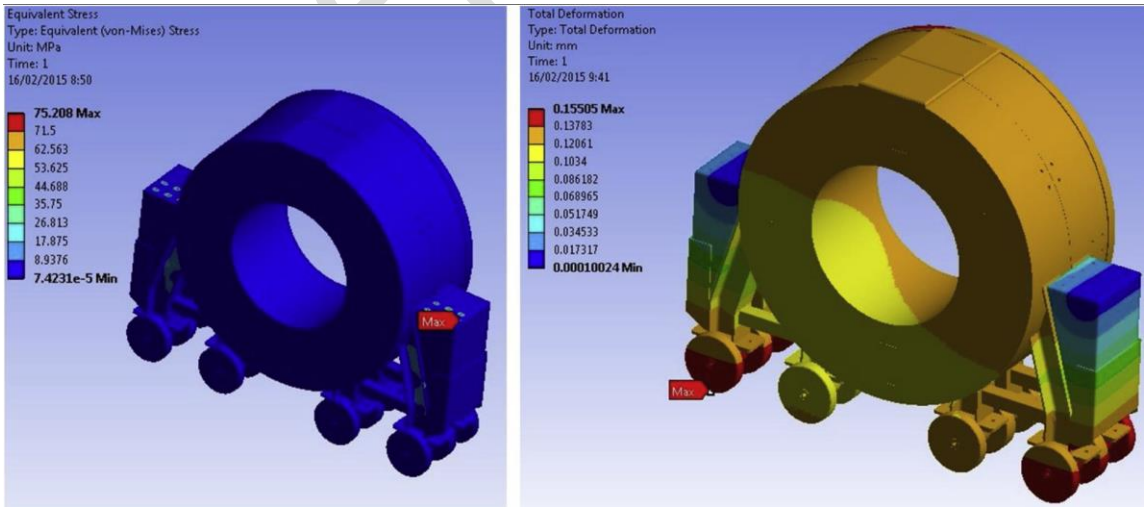

Figure 19 Von Misses stress and total deformation at the mobile front shielding.

Linearization of stresses has been applied in 4 lines of the mobile front shielding as shown in Fig. 20. The results are shown in Table 4, where the Safety Factor is the ratio between the Allowable Stress and the Stress Load. All the lines fulfil the requirements of the ASME code.

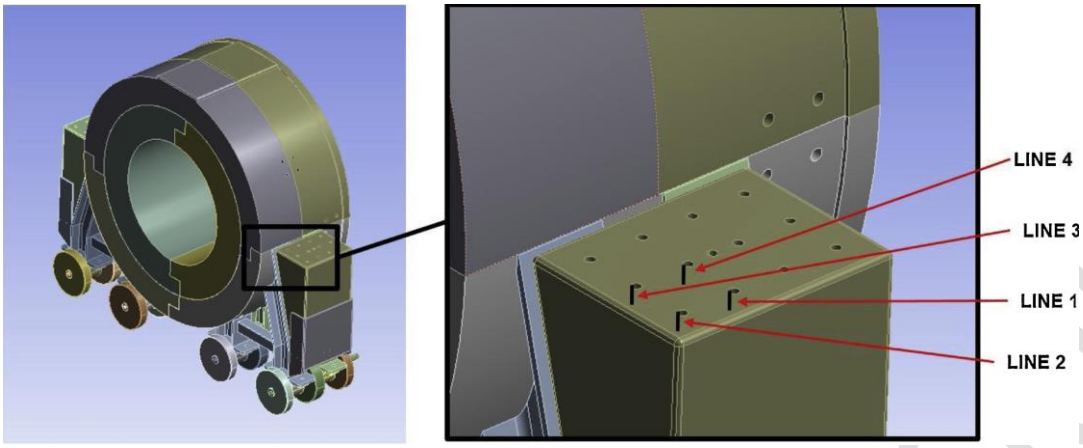

Figure 20 Lines where linearization of stresses has been applied in the mobile front shielding.

Table 4 Evaluation of protection against plastic collapse for the mobile shielding.

Line	Stress Load	Allowable Stress	Safety Factor
1	P_m=15.5 MPa	S=118 MPa	7.6
	P_L+P_b=57.3 MPa	1.5S=177 MPa	3.1
2	P_m=15 MPa	S=118 MPa	7.9
	P_L+P_b=59 MPa	1.5S=177 MPa	3
3	P_m=17.4 MPa	S=118 MPa	6.8
	P_L+P_b=65.1 MPa	1.5S=177 MPa	2.7
4	P_m=13.7 MPa	S=118 MPa	8.6
	P_L+P_b=55.1 MPa	1.5S=177 MPa	3.2

5. Manufacturing

The half rings of the iron shielding have been manufactured from low alloy steel S235 plates with a thickness of 280 mm. These plates have been bent in several stages with a stress releasing process in between, allowing to reach the inner bending radius of 869 mm (Fig. 21). Finally, the half rings have been machined in a vertical lathe and a milling machine, obtaining a final thickness of 250 mm and the detailed geometry required for each of them (Fig. 22).

Figure 21 Iron half ring after bending.

Figure 22 Iron half ring in the milling machine.

The aluminum tanks have been manufactured from Al 5083 alloy sheets of different thicknesses, allowing a minimum thickness of 10 mm after machining stages. These sheets have been bent, machined and welded together (Fig. 23). After that, the tanks have been filled with pieces of high density polyethylene PE-HMW 500, machined to their final geometry. Aluminum internal ribs have been welded, reinforcing the tanks (Fig. 24). The tanks have been closed with their outer cylindrical aluminum sheets, assembled to the tanks by means of tack welding and bolted joints. The tanks are not sealed, allowing the exit of gases that will be generated in the polyethylene due to radiation.

Figure 23 Aluminum tank during the welding stage.

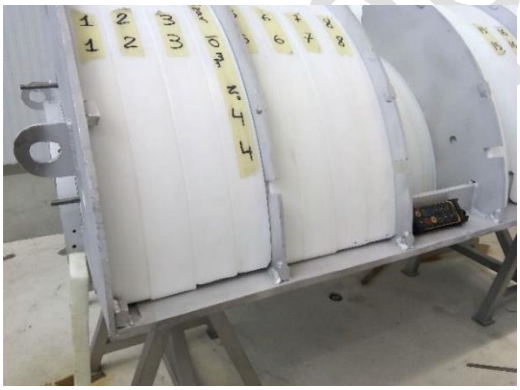

Figure 24 Filling of the tanks with high density polyethylene.

The mobile trolleys are composed of a structure made from low alloy steel S235 plates and containing a quarter of the iron shielding ring. The plates have been welded together and machined in a milling machine. The polyethylene PE-HMW 500 shielding has been fixed to the structure by means of bolted joints. The trolleys have 2 axes with 3 wheels each of them, machined from austenitic stainless steel 316 bars. One of the axes can be rotated by a gear motor in order to move the trolley (Fig. 25).

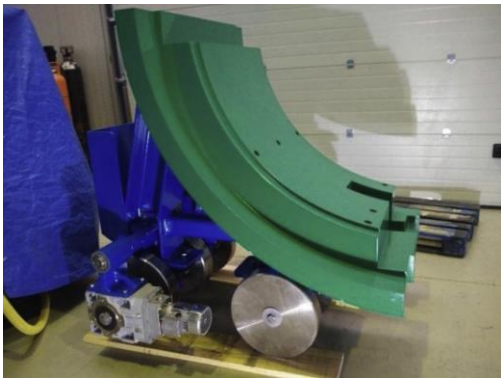

Figure 25 One of the mobile trolleys after manufacturing and assembly.

The base plates have been manufactured from austenitic stainless steel 316 sheets that have been machined to their final dimensions (Fig. 26).

Figure 26 Central base plate after machining.

6. Inspections and acceptance tests

Before the acquisition of materials, dedicated chemical analyses of the low alloy steel S235 and the aluminum alloy Al 5083 were performed to ensure that the impurities of Zn, Co and Cs were below the specified limits. The values obtained have been crosschecked with the materials certificates when the impurities quantities appeared in them.

During the manufacturing stage, the dimensions of the components and the quality of the welding have been controlled and verified issuing dimensional control certificates and welding certificates at intermediate stages of manufacturing and at the end of the whole process.

Two final acceptance tests have been carried out: an assembly and alignment test, and a realignment test.

The assembly and alignment test consisted of mounting together all the components of the beam dump shielding in a room reproducing the same constraints as in the final location in Rokkasho, Japan. These constraints were a bridge crane rotated 20º from the axial direction of the assembly with limited displacement range and a simulated wall over which the components hanging by the crane had to pass. (Fig. 27).

Figure 27 Components passing over the simulated wall.

During the test, the installation and alignment of the base plates with adjusting screws and mortar filling was proved (Fig. 28). After the assembly of the fixed iron shielding, the aluminum tanks and the beam dump cartridge, alignment of the beam dump cartridge with laser tracker was done, proving that the required accuracy of ±0.1 mm can be achieved. Finally, the remaining components were installed to check that the whole assembly process could be performed (Fig. 29).

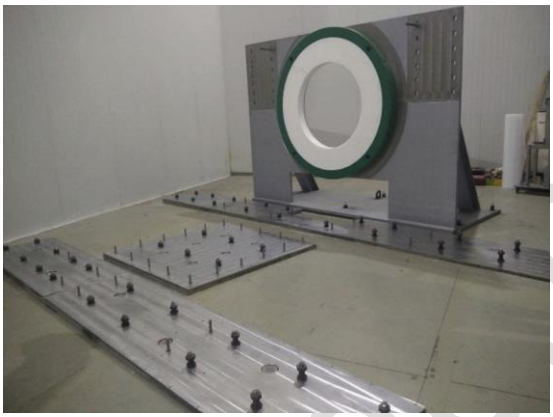

Figure 28 Installation of the base plates.

Figure 29 Assembly test of the beam dump shielding.

The realignment test consisted in removing the upper parts of the mobile shielding, opening the mobile trolleys and performing a realignment of the beam dump cartridge to ensure that, after installation, the access to the beam dump cartridge and its realignment were possible (Fig. 30).

Figure 30 Realignment of the beam dump cartridge.

After the performance of the acceptance tests, all the components were dismounted in order to be packed and shipped to their final destination. At this stage, the coordinates of the CCRs (Corner Cube Reflectors) of all the components were recorded with laser tracker in order to be used as a reference in the final assembly.

7. Lessons learned

During the design, analysis, manufacturing and acceptance tests of the beam dump shielding, several lesson have been learnt. The more important ones are listed below:

- It is better to separate the function of supporting the beam dump cartridge from the function of shielding the radiation. In this design, this has not been implemented, but it would ease the dimensional requirements for the whole shielding. Future beam dump shieldings for potential neutron sources are highly advised to follow this lesson.

- It is difficult to acquire aluminum sheets with impurities of Zn lower than the values specified.

- The first approach for the levelling of the base plates was to use small shims in some positions under the plates. The final solution with levelling bolts and mortar filling represents a clear improvement, allowing a better position accuracy, a better distribution of shielding loads and an easier assembly of the base plates.

- The use of chemical anchors instead of mechanical ones is advised in the stoppers, plates and structural supports that are planned to be dismounted and mounted frequently. The chemical anchors will have a permanent threaded bar installed allowing frequently disassembly and assembly of the fixed elements, while the mechanical anchors must be dismounted with the fixed elements or loosened. Taking into account that the repeatability in the use of mechanical anchors is limited, the chemical anchors are a better choice.

- The filling of the aluminum tanks with polyethylene instead of water allowed to lower the requirements in the manufacture of the tanks, since they no longer had to be watertight or comply with a strict welding code like ASME.

- Much of the difficulty of the shielding design comes from the limited capacity of the bridge crane in the building. So, for future designs, it is highly advised to foresee a bridge crane with a load capacity according to the total weight of the shield.

8. Conclusions

A beam dump shielding for the IFMIF LIPAc accelerator has been devised, designed, analyzed, manufactured and tested.

The beam dump shielding fulfils the main requirement, to attenuate both the radiation produced during accelerator operation and the residual radiation. Other requirements, including reduced own contribution to radiation, structural integrity, dimensional tolerances, alignment capability, commissioning, decommissioning and regulation, have also been fulfilled.

Inspections and final acceptance tests have been performed ensuring the accomplishment of all the requirements mentioned.

Declaration of Competing Interest

The authors declare that they have no known competing financial interests or personal relationships that could have appeared to influence the work reported in this paper.

Acknowledgment

This work has been supported by the Spanish Government in the frame of the Broader Approach Agreement.

References:

[1] J. Knaster, et al. IFMIF, the European-Japanese efforts under the broader approach agreement towards a Li(d,xn) neutron source: current status and future options. Nucl. Mater. Energy (2016), pp. 1-9

[2] P. Cara, et al. The linear IFMIF prototype accelerator (LIPAC) design development under the European-Japanese collaboration. Proc. IPAC, 16 (2016), pp. 985-988

[3] D. Gex, P.Y. Beauvais, B. Brañas, et al. Engineering progress of the linear IFMIF prototype accelerator (LIPAc). Fus. Eng. Des., 88 (2013), pp. 2497-2501

[4] B. Brañas, F. Arranz, O. Nomen, et al. The LIPAc beam dump. Fusion Eng. Des., 127 (2018), pp. 127-138

[5] B. Brañas, D. Iglesias, F. Arranz, G. Barrera, N. Casal, M. García, et al. Design of a beam dump for the IFMIF–EVEDA accelerator. Fus. Eng. Des., 84 (2–6) (2009), pp. 509-513

[6] M. García, F. Ogando, et al. Optimized design of local shielding for the IFMIF/EVEDA beam dump. SATIF 10. Workshop Proceedings, Geneva, Switzerland 2–4 June (2010)

[7] O. Nomen, J.I. Martínez, F. Arranz, et al. Detailed mechanical design of the LIPAc beam dump radiological shielding. Fus. Eng. Design, 88 (2013), pp. 2723-2727

[8] F. Ogando, B. Brañas, et al. Radiological design and evaluation of the LIPAc beam dump shield

Fus. Eng. Des. (2019). To be submitted to, Available on request to corresponding author

[9] O. Nomen, B. Brañas, F. Ogando, et al. Lead shutter for the IFMIF LIPAc accelerator. Nucl. Instrum. Methods Phys. Res. A, 901 (2018), pp. 69-75

[10] ASME Boiler and Pressure Vessel Code, Section VIII, Division 2, Alternative Rules, Rules for Construction of Pressure Vessels. 2008ª. Addenda. (2008)

[11] K. Shinto, et al. Seismic Requirements for Installation of Components in Japan, IFMIF-EVEDA Report. (2012). Available on request to corresponding author

[12] P. Beynel, P. Maier, H. Schonbacher. Compilation of Radiation Damage Test Data. Pt. 3. Materials Used Around High-energy Accelerators. CERN-82-10, CERN-YELLOW-82-10. (1982)